

Carbon–Carbon Coupling in Dinuclear Cycloaurated Complexes Containing Bridging 2-(Diphenylphosphino)phenyl or 2-(Diethylphosphino)phenyl. Role of the Axial Ligand and the Fine Balance between Gold(II)–Gold(II) and Gold(I)–Gold(III)

Martin A. Bennett,* David C. R. Hockless, A. David Rae, Lee L. Welling, and Anthony C. Willis

Research School of Chemistry, Australian National University, Canberra, Australian Capital Territory 0200, Australia

Received September 11, 2000

Reactions of the homovalent bis(benzoato)digold(II) complexes $[\text{Au}^{\text{II}}_2(\text{O}_2\text{CPh})_2(\mu\text{-}2\text{-C}_6\text{H}_4\text{-PR}_2)_2]$ ($\text{R} = \text{Ph}$ (**1a**), Et (**1b**)) with the anions CH_3^- , C_6F_5^- , and SCN^- have been investigated. Dimethylmagnesium gives the stable heterovalent complexes $[\text{Au}^{\text{I}}(\mu\text{-}2\text{-C}_6\text{H}_4\text{PR}_2)_2\text{Au}^{\text{III}}(\text{CH}_3)_2]$ ($\text{R} = \text{Ph}$ (**2a**), Et (**2b**)), whereas (pentafluorophenyl)lithium gives the homovalent complexes $[\text{Au}^{\text{II}}_2(\text{C}_6\text{F}_5)_2(\mu\text{-}2\text{-C}_6\text{H}_4\text{PR}_2)_2]$ ($\text{R} = \text{Ph}$ (**3a**), Et (**3b**)). On prolonged heating in toluene, the latter rearrange to give predominantly dinuclear bis(pentafluorophenyl)digold(I) complexes of the corresponding (2,2'-biphenyl)bis(tertiary phosphines) $[\text{Au}^{\text{I}}_2(\text{C}_6\text{F}_5)_2(\mu\text{-}2,2'\text{-R}_2\text{PC}_6\text{H}_4\text{C}_6\text{H}_4\text{-PR}_2)_2]$ ($\text{R} = \text{Ph}$ (**4a**), Et (**4b**)), resulting from coupling of the $\text{C}_6\text{H}_4\text{PR}_2$ units. Minor products of these rearrangements are the zwitterionic heterovalent complexes $[(\text{C}_6\text{F}_5)_2\text{Au}^{\text{III}}(\mu\text{-}2\text{-C}_6\text{H}_4\text{-PR}_2)_2\text{Au}^{\text{I}}]$ ($\text{R} = \text{Ph}$ (**5a**), Et (**5b**)). The structure of **5a** differs from that of **2a** by rotation of one of the bridging 2- $\text{C}_6\text{H}_4\text{PPh}_2$ groups through 180° . Precursors to **4a/5a** and **4b/5b** have been detected by ^{31}P NMR spectroscopy and tentatively assigned the heterovalent structures $(\text{C}_6\text{F}_5)\text{Au}^{\text{I}}(\mu\text{-}2\text{-R}_2\text{PC}_6\text{H}_4)\text{Au}^{\text{III}}(\text{C}_6\text{F}_5)(\eta^2\text{-}2\text{-C}_6\text{H}_4\text{PR}_2)_2]$ ($\text{R} = \text{Ph}$ (**6a**), Et (**6b**)), in which one $\text{C}_6\text{H}_4\text{-PR}_2$ group bridges the two gold atoms while the other binds as a bidentate chelate ligand to gold(III). The S-bonded bis(thiocyanato) complexes $[\text{Au}^{\text{II}}_2(\text{SCN})_2(\mu\text{-}2\text{-C}_6\text{H}_4\text{PR}_2)_2]$ ($\text{R} = \text{Ph}$ (**8a**), Et (**8b**)) formed from **1a** or **1b** and KSCN undergo C–C coupling more rapidly than the C_6F_5 compounds to give $[\text{Au}^{\text{I}}_2(\text{SCN})_2(\mu\text{-}2,2'\text{-R}_2\text{PC}_6\text{H}_4\text{C}_6\text{H}_4\text{PR}_2)_2]$ ($\text{R} = \text{Ph}$ (**10a**), Et (**10b**)) via the detectable heterovalent intermediates **9a** or **9b**, which are analogues of **6a** and **6b**. The X-ray structures of complexes **2a**, **3a**, **4a**, **4b**, **5a**, and **10b** have been determined. The gold–gold separations in **2a**, **3a**, and **5a** are respectively 2.8874(4), 2.6139(4), and 2.931(1)/2.921(1) Å (for independent molecules), the shorter distance in **3a** corresponding to a covalent metal–metal bond. In **4a** and **10b** the torsion about the central C–C bond of the biphenyl backbone results in a *syn* configuration for the Au–X ($\text{X} = \text{C}_6\text{F}_5$, SCN) fragments and a close intramolecular aurophilic contact between the gold atoms ($r(\text{Au}\cdots\text{Au}) = 3.0688(8)$ Å (**4a**), 3.0853(9) Å (**10b**)), whereas in **4b** the Au– C_6F_5 units adopt an *anti* configuration relative to the biphenyl fragment, leading to a nonbonding gold–gold separation of 5.3469(7) Å. The differences in behavior of digold(II) complexes $[\text{Au}_2\text{X}_2(\mu\text{-}2\text{-C}_6\text{H}_4\text{PR}_2)_2]$ as the axial anionic ligand X is varied and the pathway of the intramolecular C–C coupling reaction are discussed.

Introduction

We have shown previously that the carbanions $(2\text{-C}_6\text{H}_4\text{PR}_2)^-$ ($\text{R} = \text{Ph}$, Et) form digold(I) complexes $[\text{Au}_2(2\text{-C}_6\text{H}_4\text{PR}_2)_2]$, in which two linearly coordinated gold(I) atoms are held in close proximity. These compounds undergo oxidative addition with halogens or dibenzoyl peroxide to give the symmetrical digold(II) complexes $[\text{Au}_2\text{X}_2(2\text{-C}_6\text{H}_4\text{PR}_2)_2]$ ($\text{X} = \text{Cl}$, Br , I , O_2CPh), which contain a pair of planar-coordinated gold(II) atoms connected by a direct metal–metal bond.^{1–3} Gold(I) and gold(II) complexes of similar geometry are formed by many other 1,3-bifunctional ligands;⁴ those with

bis(ylides), $[\text{R}_2\text{P}(\text{CH}_2)_2]^-$ ($\text{R} = \text{Me}$, Et , Ph), have attracted particular attention.^{4–9} Uniquely, however, the digold(II) dihalide complexes containing 2- $\text{C}_6\text{H}_4\text{PR}_2$

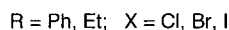
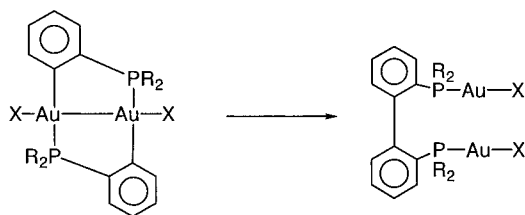
(1) Bennett, M. A.; Bhargava, S. K.; Griffiths, K. D.; Robertson, G. B.; Wickramasinghe, W. A.; Willis, A. C. *Angew. Chem., Int. Ed. Engl.* **1987**, *26*, 258.

(2) Bennett, M. A.; Bhargava, S. K.; Griffiths, K. D.; Robertson, G. B. *Angew. Chem., Int. Ed. Engl.* **1987**, *26*, 260.

(3) Bennett, M. A.; Bhargava, S. K.; Hockless, D. C. R.; Welling, L. L.; Willis, A. C. *J. Am. Chem. Soc.* **1996**, *118*, 10469.

(4) Articles by: Laguna, A. In *Gold, Progress in Chemistry, Biotechnology and Technology*; Schmidbaur, H., Ed.; Wiley: Chichester, U.K., 1999; Chapter 12, p 349. Fackler, J. P.; van Zyl, W. E.; Prihoda, B. A. *Ibid.*, Chapter 20, p 795.

Scheme 1



isomerize by coupling of the carbanions at the dimetal center to give digold(I) complexes of the corresponding 2,2'-biphenyl-substituted ligands, $[\text{Au}_2\text{X}_2(\mu\text{-}2\text{-R}_2\text{-PC}_6\text{H}_4\text{C}_6\text{H}_4\text{PR}_2)]$ (Scheme 1). This reductive elimination, in which a C–C bond is formed at the expense of two Au–C bonds, occurs readily for $X = \text{I, Br, Cl}$ but not at all for $X = \text{O}_2\text{CPh, O}_2\text{CMe, ONO}_2$; for $R = \text{Ph}$, the first-order rate constants for thermal isomerization decrease in the order $X = \text{I} > \text{Br} > \text{Cl}$.³ Since C–C coupling seemed to be favored by less electron-withdrawing anionic ligands, we have investigated the behavior of $\text{Au}^{\text{II}}_2(2\text{-C}_6\text{H}_4\text{PR}_2)_2$ complexes containing the more covalently binding, electron-releasing anionic ligands CH_3 , C_6F_5 , and SCN . These studies have thrown light on the likely pathway of the C–C coupling reaction.

Results

The new members of the $\text{Au}_2\text{X}_2(\text{C}_6\text{H}_4\text{PR}_2)_2$ series are conveniently obtained by anation of the bis(benzoato) complexes $[\text{Au}_2(\text{O}_2\text{CPh})_2(\mu\text{-}2\text{-C}_6\text{H}_4\text{PR}_2)_2]$ ($R = \text{Ph}$ (**1a**), Et (**1b**)), as outlined in Scheme 2.³ Attempts to prepare the dimethyl compound by reaction of methyl lithium with either **1a** or $[\text{Au}_2(\mu\text{-}2\text{-C}_6\text{H}_4\text{PR}_2)_2]$ gave mainly the digold(I) precursor $[\text{Au}_2(\mu\text{-}2\text{-C}_6\text{H}_4\text{PR}_2)_2]$ as a result of reduction. However, from reaction of **1a** or **1b** with a slight excess of dimethylmagnesium, colorless solids of empirical formula $\text{Au}_2(\text{CH}_3)_2(\text{C}_6\text{H}_4\text{PR}_2)_2$ were isolated in 70–80% yield. The ^1H NMR spectra in CD_2Cl_2 show a six-proton doublet resonance close to δ 0 due to the Au– CH_3 groups, and the highest mass peaks in the FAB-mass spectra correspond in each case to the loss of one methyl group from the unobserved parent ion. The $^{31}\text{P}\{^1\text{H}\}$ NMR spectra consist of a pair of equally intense doublets in the region δ 6–35 ($^2J_{\text{PP}} = 27.5$ Hz), arising from inequivalent phosphorus atoms, and thus are inconsistent with a symmetrical digold(II) structure. The spectroscopic data are, however, compatible with the unsymmetrical structures **2a** ($R = \text{Ph}$) and **2b** ($R = \text{Et}$), and this conclusion has been confirmed by the single-crystal X-ray structure of **2a**, which is shown in Figure 1 together with the atom labeling. Selected bond distances and angles are given in Table 1.

The $2\text{-C}_6\text{H}_4\text{PPh}_2$ groups bridge a pair of gold atoms, one of which, Au(1), is trivalent with approximately

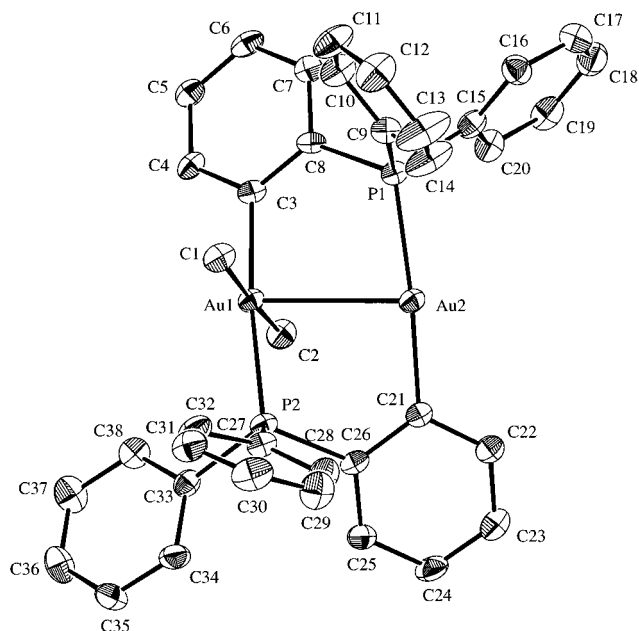
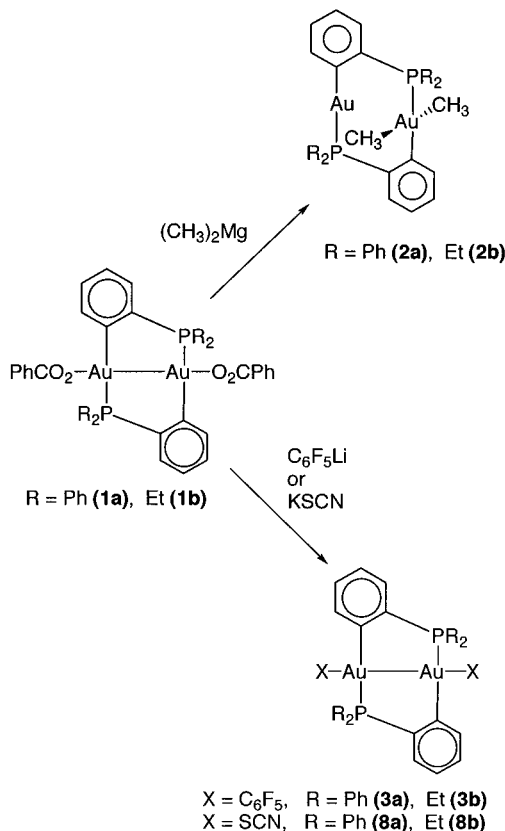


Figure 1. Molecular structure of **2a** with atom labeling. Thermal ellipsoids show 30% probability levels; hydrogen atoms have been omitted for clarity.

Scheme 2



planar coordination; the other, Au(2), is univalent and its coordination geometry is close to linear. The methyl groups on Au(1) are mutually trans, the Au–C bond lengths (2.089(8) Å, 2.126(8) Å) being similar to those observed for the *trans*-methyl groups in the monomeric gold(III) complex $[\text{Au}(\text{CH}_3)_3(\text{PPh}_3)]$ (2.057(27)–2.168(22) Å).¹⁰ Although the separation between the metal atoms in **2a** (2.8874(4) Å) is larger than that in the symmetrical digold(II) complexes $[\text{Au}_2\text{X}_2(2\text{-C}_6\text{H}_4\text{PR}_2)_2]$ (2.593

(5) Grohmann, A.; Schmidbauer, H. In *Comprehensive Organometallic Chemistry II*; Wardell, J., Abel, E. W., Stone, F. G. A., Wilkinson, G., Eds.; Pergamon: Oxford, U.K., 1995; Vol. 3, p 1.

(6) Fackler, J. P., Jr. *Polyhedron* **1997**, *16*, 1.

(7) Schmidbauer, H.; Grohmann, A.; Olmos, M. E. In *Gold, Progress in Chemistry, Biochemistry and Technology*; Schmidbauer, H., Ed.; Wiley: Chichester, U.K., 1999; Chapter 18, p 648.

(8) Laguna, A.; Laguna, M. *Coord. Chem. Rev.* **1999**, *193–195*, 837.

(9) Laguna, M.; Cerrada, E. In *Metal Clusters in Chemistry*; Braunstein, P., Oro, L. A., Raithby, P. R., Eds.; Wiley-VCH: Weinheim, Germany, 1999; Vol. 1, p 459.

Table 1. Selected Bond Lengths (Å) and Angles (deg) for [Au^{I,III}₂Me₂(2-C₆H₄PPh₂)₂] (2a)

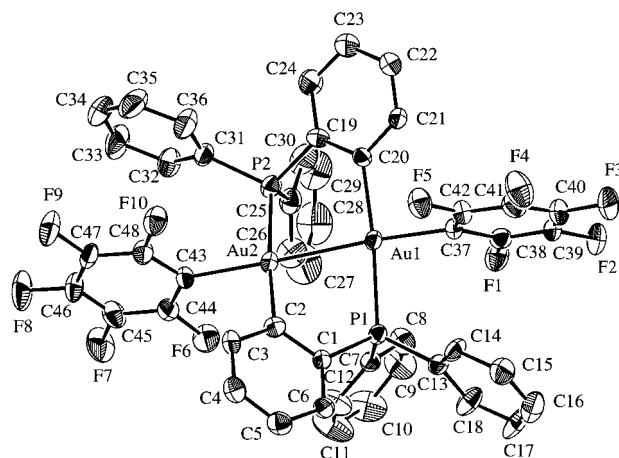
Au(1)–P(2)	2.347(2)	Au(2)–P(1)	2.308(2)
Au(1)–C(1)	2.089(8)	Au(1)–C(2)	2.126(8)
Au(1)–C(3)	2.055(7)	Au(2)–C(21)	2.053(7)
Au(1)⋯Au(2)	2.8874(4)	P–C	1.807(8)–1.840(8)
Au(2)–Au(1)–P(2)	80.86(5)	Au(2)–Au(1)–C(1)	95.2(3)
Au(2)–Au(1)–C(2)	86.2(2)	Au(2)–Au(1)–C(3)	93.8(2)
P(2)–Au(1)–C(1)	96.0(2)	P(2)–Au(1)–C(2)	89.1(2)
P(2)–Au(1)–C(3)	174.0(2)	C(1)–Au(1)–C(2)	174.9(3)
C(1)–Au(1)–C(3)	87.2(3)	C(2)–Au(1)–C(3)	87.8(3)
Au(1)–Au(2)–P(1)	81.81(5)	Au(1)–Au(2)–C(21)	92.6(2)
P(1)–Au(2)–C(21)	171.7(2)		

Å (av) for R = Ph, X = I;² 2.5243(7) Å for R = Et, X = O₂CPh³), the possibility of a donor–acceptor interaction (Au(I)→Au(III)) clearly cannot be excluded. Dimethyl-digold bis(ylide) complexes analogous to **2a** have been prepared,^{11,12} but no structures have been determined. The closest analogue to **2a** in the bis(ylide) series appears to be the dibromo complex [Au^I{μ-(CH₂)₂PPh₂}₂-Au^{III}Br₂], in which the metal–metal distance is 3.061(2) Å.¹³

Examination in situ of the reaction mixture of **1a** and (CH₃)₂Mg by ³¹P{¹H} NMR spectroscopy showed the presence of a sharp singlet at δ 2.7 in addition to the doublets due to **2a**. After a few hours at room temperature, the singlet had disappeared, leaving **2a** as the only phosphorus-containing product. The chemical shift of the singlet is in the region expected for the symmetrical digold(II) complexes;³ hence, this peak may be due to the symmetrical digold(II) precursor [(CH₃)₂Au(μ-2-C₆H₄PPh₂)₂Au(CH₃)]. Attempts to cleave selectively one of the methyl groups of **2a** with benzoic acid led only to the bis(benzoato)digold(II) complex together with some digold(I) precursor.

Treatment of compound **1a** with phenyllithium (2 equiv) gave a yellow solution whose ³¹P{¹H} NMR spectrum showed a sharp singlet at δ –1.1 and a pair of doublets at δ 34.5 and 13.8 (²J_{PP} = 28.1 Hz) indicative of the presence of the digold(II) complex [(C₆H₅)Au(μ-2-C₆H₄PPh₂)₂Au(C₆H₅)] and its gold(I)–gold(III) isomer [Au(μ-2-C₆H₄PPh₂)₂Au(C₆H₅)₂]. Attempted isolation caused gradual decomposition to unidentified species.

The bis(pentafluorophenyl)digold(II) complexes [Au₂(C₆F₅)₂(μ-2-C₆H₄PR₂)₂] (R = Ph (**3a**), Et (**3b**)) were obtained in high yield as yellow, air-stable, crystalline solids from the reaction of C₆F₅Li with **1a** and **1b**, respectively. Both complexes show parent ion peaks in their FAB-mass spectra and singlets in the region δ –6 to –8 in their ³¹P{¹H} NMR spectra, no coupling to ¹⁹F being evident. The structure of **3a**, determined by single-crystal X-ray analysis, is shown in Figure 2 together with the atom-labeling scheme; selected bond lengths and angles are given in Table 2. The structure is similar to those of [Au₂I₂(2-C₆H₄PPh₂)₂]² and [Au₂(O₂CPh)₂(2-C₆H₄PET₂)₂],³ the coordination geometry about each gold atom being close to planar with the C₆F₅ groups lying on the gold–gold axis. The gold(II)–gold(II) separation in **3a**, 2.6139(4) Å, is greater than the corresponding

**Figure 2.** Molecular structure of **3a** with atom labeling. Thermal ellipsoids show 30% probability levels; hydrogen atoms have been omitted for clarity.**Table 2. Selected Bond Lengths (Å) and Angles (deg) for [Au^{II}₂(C₆F₅)₂(2-C₆H₄PPh₂)₂] (3a)**

Au(1)–P(1)	2.331(2)	Au(2)–P(2)	2.323(2)
Au(1)–C(20)	2.088(8)	Au(2)–C(2)	2.076(8)
Au(1)–C(37)	2.103(8)	Au(2)–C(43)	2.119(8)
Au(1)⋯Au(2)	2.6139(4)	P–C	1.790(9)–1.816(8)
C–F	1.326(9)–1.35(1)		
Au(2)–Au(1)–P(1)	80.80(5)	Au(2)–Au(1)–C(20)	93.3(2)
Au(2)–Au(1)–C(37)	168.3(2)	P(1)–Au(1)–C(20)	171.7(2)
P(1)–Au(1)–C(37)	94.9(2)	C(20)–Au(1)–C(37)	91.9(3)
Au(1)–Au(2)–P(2)	83.89(6)	Au(1)–Au(2)–C(2)	91.0(2)
Au(1)–Au(2)–C(43)	176.6(2)	P(2)–Au(2)–C(2)	174.5(2)
P(2)–Au(2)–C(43)	93.1(2)	C(2)–Au(2)–C(43)	92.1(3)

distances in these compounds (2.593 Å (av) and 2.5243(7) Å, respectively), reflecting the effect of the less electron-withdrawing C₆F₅ ligand in the axial position. The gold(II)–gold(II) distance is also less than those in the closely related bis(ylide) complexes [Au₂Y₂{μ-(CH₂)₂-PPh₂}₂] (2.677(1) Å for Y = C₆F₅; 2.679(1) Å for Y = CF₃),¹⁴ as a consequence of the smaller size of the bridging group in the (2-diphenylphosphino)phenyl complex. The Au–C₆F₅ bond lengths in **3a** (2.103(8), 2.119(8) Å) seem to fall in the range between those in [Au₂(C₆F₅)₂{μ-(CH₂)₂PPh₂}₂] (2.145(8)–2.164(7) Å) and those in [Au(C₆F₅)₄][–] (2.075(11)–2.084(11) Å).¹⁴

The lability of the axial pentafluorophenyl ligands is similar to that of the anionic ligands in the parent Au₂X₂(2-C₆H₄PR₂)₂ compounds.³ The ³¹P{¹H} NMR spectra of solutions in dichloromethane containing approximately equal amounts of **3b** and **1b**, measured as soon as possible after mixing, show an AB pattern (δ_A 7.7, δ_B –2.5, J_{AB} = 66 Hz) attributable to the species [(C₆F₅)Au(μ-2-C₆H₄PET₂)₂(O₂CPh)]. Mixtures of **3b** and [Au₂I₂(μ-*o*-C₆H₄PET₂)₂] behave similarly, the mixed-ligand species [(C₆F₅)Au(μ-2-C₆H₄PET₂)₂AuI] being characterized by an AB pattern at δ_A –3.5, δ_B –5.5 (J_{AB} = 67 Hz).

Although **3a** and **3b** are clearly more robust than their methyl or phenyl analogues, they are not thermodynamically stable. The changes that occur are outlined in Scheme 3. When the solutions in *d*₈-toluene were heated to 90 °C, the ³¹P{¹H} NMR spectra slowly changed. After 5 h, the solution of **3a** showed a pair of

(10) Stein, J.; Fackler, J. P., Jr.; Pappazios, C.; Chen, H.-W. *J. Am. Chem. Soc.* **1981**, *103*, 2192.

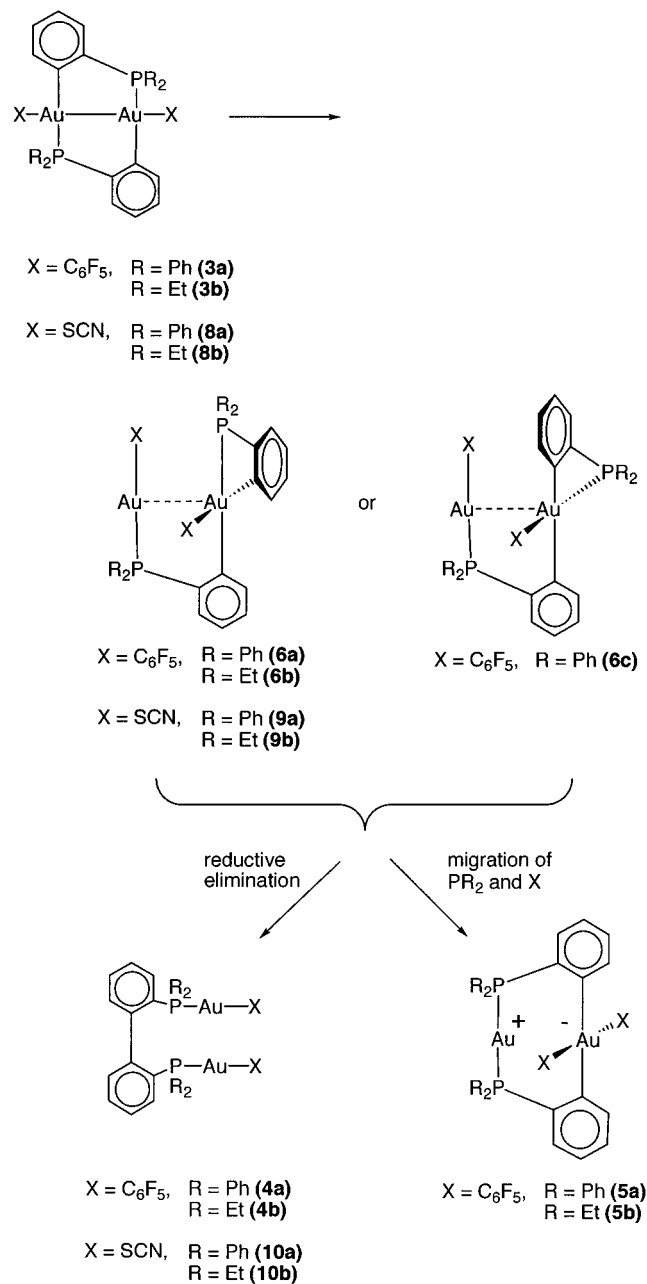
(11) Schmidbaur, H.; Franke, R. *Inorg. Chim. Acta* **1975**, *13*, 85.

(12) Schmidbaur, H.; Hartmann, C.; Riede, J.; Huber, B.; Müller, G. *Organometallics* **1986**, *5*, 1652.

(13) Raptis, R. G.; Porter, L. C.; Emrich, R. J.; Murray, H. H.; Fackler, J. P., Jr. *Inorg. Chem.* **1990**, *29*, 4408.

(14) Murray, H. H.; Fackler, J. P., Jr.; Porter, L. C.; Briggs, D. A.; Guerra, M. A.; Lagow, R. J. *Inorg. Chem.* **1987**, *26*, 357.

Scheme 3



doublets at δ 44.0 and -61.8 ($J_{PP} = 13.4$ Hz) in addition to the singlet due to unchanged starting material. Over a further 20 h these peaks disappeared and were replaced by approximate triplets at δ 36.3 and 32.8, the separation in both cases being 6.3 Hz; after 48 h these were the only observable signals, the ratio being 7:1. The compounds responsible for these signals were separated by fractional crystallization and identified by X-ray crystallography. The main product was $[Au_2(C_6F_5)_2(\mu-2,2'-Ph_2PC_6H_4C_6H_4PPh_2)]$ (**4a**), the bis(pentafluorophenyl)digold(I) derivative of (2,2'-biphenyl)-bis(diphenylphosphine) (see below). The minor product proved to be the unprecedented zwitterionic complex $[(C_6F_5)_2Au^{III}(\mu-2-C_6H_4PPh_2)_2Au^I]$ (**5a**), whose structure is shown in Figure 3; selected bond lengths and angles are listed in Table 3. The two C_6F_5 groups and both aryl carbon atoms of the bridging 2- $C_6H_4PPh_2$ group complete approximately planar coordination about the

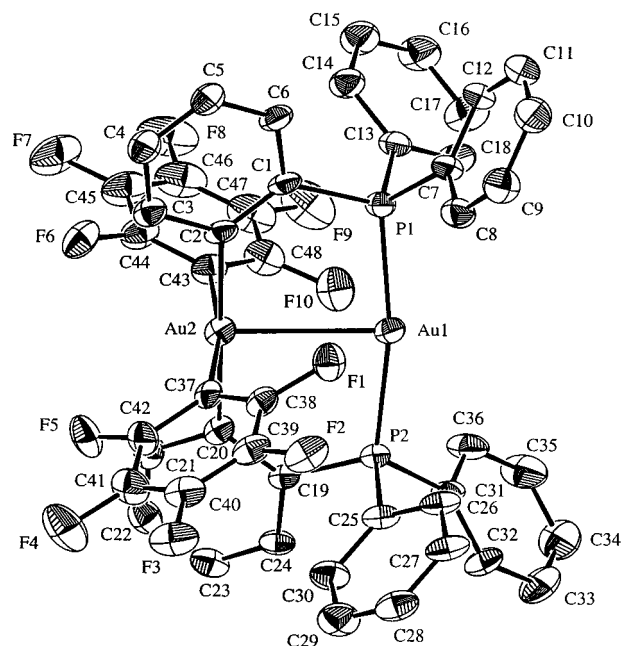


Figure 3. Molecular structure of **5a** (one of the two independent molecules) with atom labeling. Thermal ellipsoids show 30% probability levels; hydrogen atoms have been omitted for clarity.

gold(III) atom, which is therefore a monoanion, while the phosphorus atoms of the 2- $C_6H_4PPh_2$ groups are attached to the linearly coordinated gold(I) atom, which is therefore a monocation. The structure is similar to that of the dimethyl compound **2a**, except that one of the bridging $C_6H_4PPh_2$ ligands is rotated through 180° . The separations between the gold atoms, 2.931(1) and 2.921(1) Å for the two independent molecules, are significantly greater than that in the isomeric digold(II) precursor **3a**, but despite the absence of a formal covalent bond, electrostatic and donor-acceptor interactions may well be present. The Au- C_6F_5 distances (2.081(10)–2.097(10) Å) are in the same range as those in $[Au(C_6F_5)_4]^{-14}$.

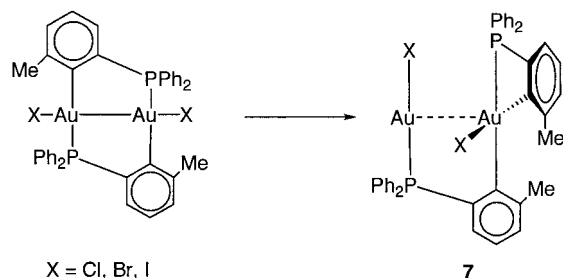
The behavior of **3b** on heating in d_8 -toluene was similar to that of **3a**. The first detectable intermediate, which showed a pair of equally intense doublets in its $^{31}P\{^1H\}$ NMR spectrum at δ 42.3 and -53.1 ($^2J_{PP} = 13.4$ Hz), transformed over a period of 48 h into two species in a 1:7 ratio showing triplet ^{31}P resonances at δ 32.9 and 30.9, the separation in each case being 6–7 Hz. The more abundant species was characterized by X-ray crystallography as $[Au_2(C_6F_5)_2(\mu-2,2'-Et_2PC_6H_4C_6H_4PEt_2)]$ (**4b**); the minor compound is assumed to be the corresponding zwitterionic complex $[(C_6F_5)_2Au^{III}(\mu-2-C_6H_4PET_2)Au^I]$ (**5b**).

Prolonged heating of **5a** in toluene did not form any **4a** and the ratios of **4a** to **5a**, or of **4b** to **5b**, in their mixtures did not change on heating; hence, the zwitterionic complexes are not precursors to the 2,2'-biphenyl compounds.

The immediate precursors to **4a/5a** and **4b/5b** could not be isolated, but the observation in each case of a highly shielded ^{31}P resonance at δ ca. -50 suggests the presence of a chelate four-membered ring,

Table 3. Selected Bond Lengths (Å) and Angles (deg) for [(C₆F₅)₂Au^{III}(μ-2-C₆H₄PPh₂)₂Au^I] (5a)

Au(1)–P(1)	2.309(5)	Au(1)–P(2)	2.308(5)
Au(2)–C(2)	2.101(12)	Au(2)–C(20)	2.098(12)
Au(2)–C(37)	2.097(10)	Au(2)–C(43)	2.081(10)
Au(1)···Au(2)	2.931(1)	P–C	1.816(12)–1.836(13)
C–F	1.344(9)–1.356(11)		
Au(3)–P(3)	2.308(5)	Au(3)–P(4)	2.320(5)
Au(4)–C(52)	2.093(12)	Au(4)–C(70)	2.088(12)
Au(4)–C(87)	2.090(10)	Au(4)–C(93)	2.087(10)
Au(3)···Au(4)	2.921(1)	P–C	1.801(13)–1.828(11)
C–F	1.344(9)–1.356(11)		
Au(2)–Au(1)–P(1)	86.4(1)	Au(2)–Au(1)–P(2)	83.2(1)
P(1)–Au(1)–P(2)	169.6(2)	Au(1)–Au(2)–C(2)	88.8(4)
Au(1)–Au(2)–C(20)	91.3(4)	Au(1)–Au(2)–C(37)	94.6(2)
Au(1)–Au(2)–C(43)	96.3(2)	C(2)–Au(2)–C(20)	179.9(4)
C(2)–Au(2)–C(37)	88.9(4)	C(2)–Au(2)–C(43)	91.4(4)
C(20)–Au(2)–C(37)	91.1(4)	C(20)–Au(2)–C(43)	88.5(4)
C(37)–Au(2)–C(43)	169.1(2)		
Au(4)–Au(3)–P(3)	84.8(1)	Au(4)–Au(3)–P(4)	83.6(1)
P(3)–Au(3)–P(4)	168.3(2)	Au(3)–Au(4)–C(52)	89.4(4)
Au(3)–Au(4)–C(70)	90.5(4)	Au(3)–Au(4)–C(87)	95.2(2)
Au(3)–Au(4)–C(93)	93.2(2)	C(52)–Au(4)–C(70)	179.2(4)
C(52)–Au(4)–C(87)	88.1(4)	C(52)–Au(4)–C(93)	91.2(4)
C(70)–Au(4)–C(87)	92.7(4)	C(70)–Au(4)–C(93)	88.0(4)
C(87)–Au(4)–C(93)	171.6(2)		

Scheme 4

M(2-C₆H₄PR₂).¹⁵ For example, the value of δ_P in [Pt(2-C₆H₄PPh₂)₂] is -52.3 ,¹⁶ and similar or even more shielded ³¹P resonances are found in related complexes of other transition elements. The ³¹P NMR spectra of the intermediates are consistent with dinuclear gold(I)–gold(III) species (**6a**, R = Ph; **6b**, R = Et) in which one C₆H₄PR₂ acts as a bidentate chelate ligand to planar-coordinated gold(III) and the other as a bridging ligand from gold(III) to linearly coordinated gold(I). This assignment is supported by the observation¹⁷ that the dihalodigold(II) complexes containing the sterically hindered bridging group 2-(diphenylphosphino)-6-methylphenyl, [Au₂X₂{μ-2-(C₆H₃-6-Me)PPh₂}₂] (X = Cl, Br, I), rearrange spontaneously in solution above -20 °C to isolable gold(I)–gold(III) complexes (Scheme 4) whose ³¹P NMR spectra resemble those of **6a** and **6b** and whose structure, **7**, has been established by X-ray crystallography in the case of X = I.

We make the arbitrary assumption that the ligand arrangement about the gold(III) atom in **6a** and **6b** is the same as that found in **7**, i.e., with C₆F₅ *trans* to the Au–C σ -bond of the four-membered ring and phosphorus *trans* to the Au–C σ -bond of the bridging C₆H₄PPh₂

group. Clearly, there is an alternative arrangement **6c** (R = Ph) in which C₆F₅ is *trans* to phosphorus and the Au–C σ -bonds of the two C₆H₄PPh₂ groups are *trans* to each other. When complex **3a** was heated in acetone instead of toluene, the solution being exposed to laboratory light, a second pair of doublets at δ 40.1 and -64.0 ($J_{PP} = 13.4$ Hz) was frequently observed in addition to the pair at δ 44.4 and -61.9 . Both pairs of doublets disappeared on continued heating as **4a** and **5a** were formed. It seems likely that this second pair of signals belongs to the alternative isomer **6c**; of course, the structural assignments for **6a** and **6c** could be reversed.

As shown in Scheme 3, the behavior of the bis-(thiocyanato)digold(II) complexes is rather similar to that of their bis(pentafluorophenyl) analogues, but the changes occur more rapidly. Treatment of complexes **1a** and **1b** with an excess of KSCN or LiSCN in acetone immediately gave orange, light-sensitive precipitates, which are assumed to be the S-bonded complexes [Au₂(SCN)₂(μ-2-C₆H₄PR₂)₂] (R = Ph (**8a**), Et (**8b**)). They show singlets in their ³¹P{¹H} NMR spectra and strong bands in their IR spectra at ca. 2100 and 690 cm⁻¹ assignable to ν (CN) and ν (CS), respectively, of S-bonded thiocyanate.¹⁸ Over a period of hours the solutions of **8a** and **8b** in CH₂Cl₂ become colorless; the singlets disappear and are replaced by a pair of doublets at δ 37–38 and δ -41 to -49 ($J_{PP} = 11$ – 12 Hz) and a singlet at δ ca. 53. The nature of the species responsible for the latter resonance is unknown, but the former can be assigned on the basis of the evidence cited above to the gold(I)–gold(III) structures **9a** and **9b**. Finally, all these signals are replaced by singlets at δ 32.0 (R = Ph) and 26.2 (R = Et), which are due to the Au–SCN complexes of 2,2'-biphenylbis(diphenylphosphine) and its diethylphosphine analogue, [Au₂(SCN)₂{μ-2,2'-R₂PC₆H₄C₆H₄PR₂}] (R = Ph (**10a**), Et (**10b**)). These have been isolated, and the structure of **10b** has been determined by single-crystal X-ray diffraction.

(15) Garrou, P. E. *Chem. Rev.* **1981**, *81*, 229.

(16) Bennett, M. A.; Berry, D. E.; Bhargava, S. K.; Ditzel, E. J.; Robertson, G. B.; Willis, A. C. *J. Chem. Soc., Chem. Commun.* **1987**, 1613.

(17) Bhargava, S. K.; Mohr, F.; Bennett, M. A.; Welling, L. L.; Willis, A. C. *Organometallics*, accepted for publication.

(18) Nakamoto, K. *Infrared and Raman Spectra of Inorganic and Coordination Compounds*, 5th ed.; Wiley-Interscience: New York, 1997; Part B, pp 116–121.

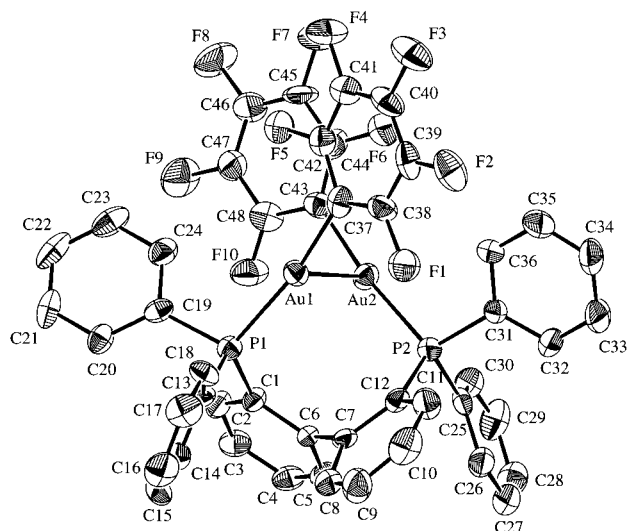


Figure 4. Molecular structure of **4a** with atom labeling. Thermal ellipsoids show 30% probability levels; hydrogen atoms have been omitted for clarity. Selected interatomic distances (Å) and angles (deg): Au(1)⋯Au(2) = 3.0688(8), Au(1)–P(1) = 2.278(3), Au(2)–P(2) = 2.285(3), Au(1)–C(37) = 2.02(1), Au(2)–C(43) = 2.04(1); P(1)–Au(1)–C(37) = 168.0(4), P(2)–Au(2)–C(43) = 172.3(4), Au(1)–Au(2)–P(2) = 87.25(9), Au(2)–Au(1)–P(1) = 89.54(9).

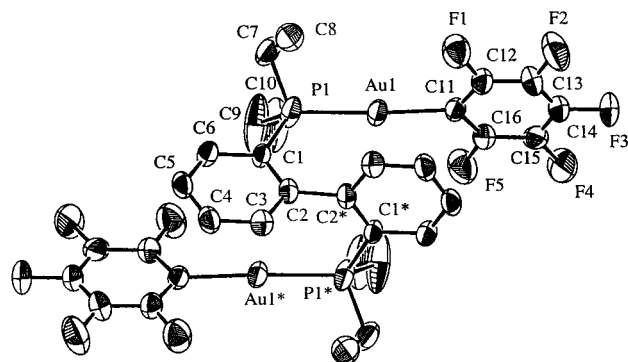


Figure 5. Molecular structure of **4b** with atom labeling; asterisked atoms are generated by the symmetry operation $-x, y, 1/2 - z$. Thermal ellipsoids show 30% probability levels; hydrogen atoms have been omitted for clarity. Selected interatomic distances (Å) and angles (deg): Au(1)⋯Au(1)* = 5.3469(7), Au(1)–P(1) = 2.271(2), Au(1)–C(11) = 2.056(7); P(1)–Au–C(11) = 176.5(3).

The structures of $[\text{Au}_2\text{X}_2(\mu\text{-}2,2'\text{-R}_2\text{PC}_6\text{H}_4\text{C}_6\text{H}_4\text{PR}_2)]$ ($\text{X} = \text{C}_6\text{F}_5$, $\text{R} = \text{Ph}$, **4a**; $\text{X} = \text{C}_6\text{F}_5$, $\text{R} = \text{Et}$, **4b**; $\text{X} = \text{SCN}$, $\text{R} = \text{Et}$, **10b**) are shown in Figures 4–6, respectively, together with the atom-labeling schemes. In all three compounds, the bis(tertiary phosphine) bridges, through phosphorus, a pair of linearly coordinated gold atoms. The biphenyl backbone is twisted about the central C–C bond, the dihedral angles between the planes of the phenyl groups being 90° (**4a**), 95° (**4b**), and 80° (**10b**). In **4a** and **10b** this torsion brings the gold atoms into fairly close contact; the separations, 3.0688(8) and 3.0853(9) Å, respectively, are in the range typical of closed-shell, attractive (aurophilic) interactions in gold(I) complexes¹⁹ and are similar to those observed in other members of the series, e.g. $[\text{Au}_2\text{Br}_2(\mu\text{-}2,2'\text{-Ph}_2\text{PC}_6\text{H}_4\text{C}_6\text{H}_4\text{PPh}_2)]$ (3.3013(5) Å),² $[\text{Au}_2\text{I}_2(\mu\text{-}2,2'\text{-Et}_2\text{PC}_6\text{H}_4\text{C}_6\text{H}_4\text{PEt}_2)]$ (3.167(1) Å),³ and $[\text{Au}_2\text{I}_2\{\mu\text{-}2,2'\text{-Ph}$

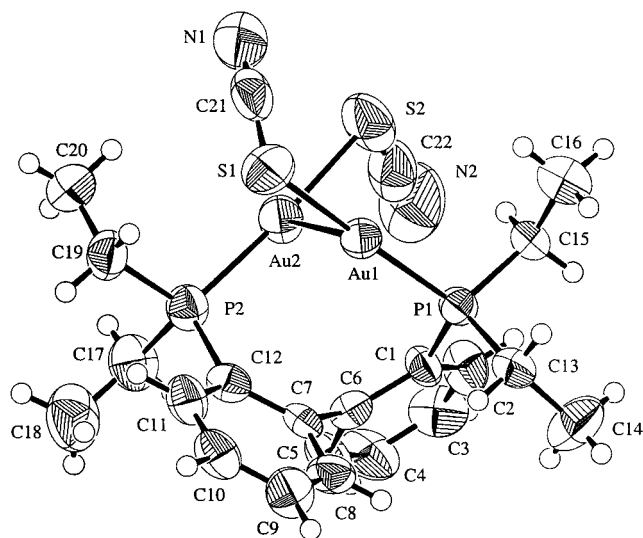


Figure 6. Molecular structure of **10b** with atom labeling. Thermal ellipsoids show 50% probability levels except for hydrogen atoms, which are drawn as circles of small radius. Selected interatomic distances (Å) and angles (deg): Au(1)⋯Au(2) = 3.0853(9), Au(1)–P(1) = 2.256(3), Au(2)–P(2) = 2.260(3), Au(1)–S(1) = 2.332(4), Au(2)–S(2) = 2.328(4), S(1)–C(21) = 1.63(2), S(2)–C(22) = 1.66(2), N(1)–C(21) = 1.18(2), N(2)–C(22) = 1.13(3); S(1)–Au(1)–P(1) = 174.5(1), S(2)–Au(2)–P(2) = 175.7(1), Au(2)–Au(1)–P(1) = 85.55(8), Au(1)–Au(2)–P(2) = 85.97(9), Au(1)–S(1)–C(21) = 98.0(6), Au(2)–S(2)–C(22) = 96.2(7), S(1)–C(21)–N(1) = 179(2), S(2)–C(22)–N(2) = 177(3).

$(\text{Et})\text{PC}_6\text{H}_4\text{C}_6\text{H}_4\text{P}(\text{Et})\text{Ph}]$ (2.9924(9) Å).²⁰ Exceptionally, the torsion in **4b** is in the opposite sense, causing the gold atoms to adopt an *anti* rather than a *syn* orientation relative to the biphenyl backbone and to be separated by 5.3469(7) Å. Presumably in **4b** the relatively weak aurophilic interaction is overcome by the lattice energy associated with a more favorable packing arrangement in the crystal.

In light of the results with the bis(pentafluorophenyl) and bis(thiocyanato) complexes, we reexamined the previously reported isomerizations of some of the dihalo complexes.³ The $^{31}\text{P}\{^1\text{H}\}$ NMR spectrum of the solution obtained by heating the iodo compound $[\text{Au}_2\text{I}_2(\mu\text{-}2\text{-C}_6\text{H}_4\text{-PEt}_2)_2]$ at 50°C in C_6D_6 for 4 h showed a pair of doublets at δ 39.3 and -62.1 ($J_{\text{PP}} = 12.6$ Hz) in addition to singlets due to the starting material at δ -11.7 and the C–C coupled product at δ 27.0. Further heating caused complete conversion into the 2,2'-biphenyl compound. In the isomerization of the $[\text{Au}_2\text{X}_2(2\text{-C}_6\text{H}_4\text{PPh}_2)_2]$ complexes, however, no corresponding intermediates could be detected.

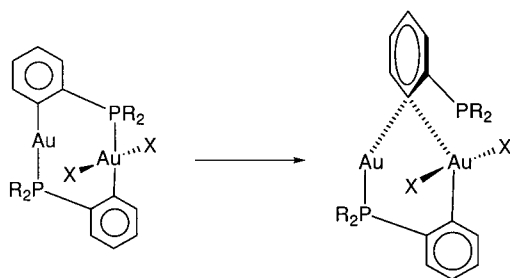
Discussion

The stability and isomerization behavior of the symmetrical, homovalent digold(II) complexes $[\text{Au}_2\text{X}_2(\mu\text{-}2\text{-C}_6\text{H}_4\text{PPh}_2)_2]$ are strongly dependent on the nature of the axial ligand X. These compounds appear to be thermodynamically stable only when X is a strongly electron-withdrawing anionic O-donor ligand such as acetate, benzoate, or nitrate. When X is a strongly

(19) Schmidbaur, H. *Gold Bull.* **1990**, *23*, 11; *Chem. Soc. Rev.* **1995**, *24*, 391.

(20) Bennett, M. A.; Welling, L. L.; Willis, A. C. Unpublished work.

Scheme 5



electron-donating carbanion, such as methyl, the homovalent compound isomerizes rapidly to the heterovalent gold(I)–gold(III) structure **2a**, without disturbing the arrangement of the bridging $C_6H_4PPh_2$ ligands. This behavior is undoubtedly associated with the high *trans* influence of methyl; i.e., the methyl ligands weaken the gold(II)–gold(II) bond by virtue of their competition for 6s-electron density.²¹ The same effect probably operates in the bis(ylide) series: the high *trans* influence of alkyl groups on the gold–gold and, more markedly, on the axial gold–halide bonds is evident in the structures of $[Au_2(X)(R)\{\mu-(CH_2)_2PPh_2\}_2]$ ($R = CH_3$, $X = Br$;²² $R = C_2H_5$, $X = I$ ²³). Further experiments will be required to determine whether the methyl groups are transferred in an intramolecular or intermolecular fashion.

We suggested previously³ that a key step in the intramolecular C–C coupling reaction of $[Au_2X_2(2-C_6H_4PR_2)_2]$ is migration of the metal–carbon bond of $C_6H_4PPh_2$ between gold atoms to generate a heterovalent intermediate and that the C–C coupling occurs by reductive elimination of two metal–carbon σ -bonds at the gold(III) center. Intermediates containing gold(I) and gold(III) resulting from such a migration have now been detected for the cases $R = Ph$, Et , $X = C_6F_5$, SCN and $R = Et$, $X = I$ and their structure established with reasonable certainty. The proposed reaction sequence leading to the C–C coupled product is depicted in Scheme 3. The favored mode of reaction for the intermediate is evidently intramolecular C–C coupling at the gold(III) center; however, it is also possible for the phosphorus atom in the four-membered ring to migrate from gold(III) to gold(I) and for the anionic ligand X to migrate from gold(I) to gold(III) to give the zwitterionic species that has been isolated and characterized in the case of $X = C_6F_5$, $R = Ph$. At least for $X = C_6F_5$, this species does not undergo reductive elimination and is not an intermediate in the C–C coupling reaction.

It is noteworthy that the C–C coupling reaction in $[Au_2X_2(2-C_6H_4PR_2)_2]$ is observed only when the axial anions (C_6F_5 , NCS , I , Br , Cl) are intermediate in electron-withdrawing ability between CH_3 and C_6H_5 on one hand and oxygen-donor ligands such as benzoate on the other. We can account for this phenomenon on the basis of our original assumption³ that each digold(II) complex is potentially in equilibrium with a heterovalent isomer that is structurally similar to the isolated dimethyl compound **2a** (Scheme 5). If the gold(III) center

is sufficiently electrophilic, the aryl group can migrate from gold(I) to gold(III) via a bridging intermediate or transition state. For ligands (X) such as halide or thiocyanate, the migration may be triggered by anion dissociation, although this seems less likely for the carbanion C_6F_5 . Bis(benzoato)digold(II) complexes possess remarkably short, and presumably strong, metal–metal bonds, e.g. 2.5243(7) Å in $[Au_2(O_2CPh)_2(\mu-2-C_6H_4PEt_2)_2]$ ³ and 2.587(1) and 2.560(2) Å for independent molecules of the bis(ylide) complex $[Au_2(O_2CPh)_2\{\mu-(CH_2)_2PPh_2\}_2]$;²⁴ hence, for anionic oxygen-donor ligands such as benzoate the heterovalent isomer may be energetically inaccessible. In contrast, for carbanionic ligands such as methyl, the heterovalent isomer is the stable form but the gold(III) center is insufficiently electrophilic to promote aryl migration.

Experimental Section

General Procedures. Syntheses were carried out under dry, prepurified nitrogen with use of standard Schlenk techniques, although the isolated solid complexes were usually air-stable. The following instruments were used for spectroscopic measurements: Varian XL-200E (1H NMR at 200 MHz, ^{19}F NMR at 188.15 MHz, ^{31}P NMR at 80.96 MHz), Varian Gemini-300 BB (1H NMR at 200 MHz, ^{31}P NMR at 121.44 MHz), VG ZAB-2SEQ (high-resolution EI and FAB mass spectra), Perkin-Elmer PE 683 and 1800 FT (infrared spectra as KBr disks, Nujol mulls or polythene disks in the ranges 4000–400 and 4000–150 cm^{-1}). The NMR chemical shifts (δ) are given in ppm relative to TMS (1H), $CFCl_3$ (^{19}F), and 85% H_3PO_4 , the first being referenced to solvent. Elemental analyses were done in-house.

Starting Materials. The compound 2- $BrC_6H_4PPh_2$ was made initially either by the reaction of $PhMgBr$ with 2- $BrC_6H_4PCl_2$ ²⁵ or by the $[PdCl_2(NCMe)_2]$ -catalyzed reaction between 2- BrC_6H_4I and Ph_2PSiMe_3 ;²⁶ later we employed the more convenient reaction of Ph_2PCl with 1,2- BrC_6H_4Li , the latter being generated from 1,2- $C_6H_4Br_2$ and $BuLi$ at $-100^\circ C$.²⁷ The compound 2- $BrC_6H_4PEt_2$ was made either from 2- $BrC_6H_4PCl_2$ and $EtMgI$ ³ or by the reaction of Et_2PCl with 1,2- BrC_6H_4Li .²⁸ Dimethylmagnesium was prepared by dioxane-induced disproportionation of CH_3MgI following the procedure described for $(Me_3SiCH_2)_2Mg$.²⁹ The complexes $[Au_2(\mu-2-C_6H_4PR_2)_2]$ and $[Au_2(O_2CPh)_2(\mu-2-C_6H_4PR_2)_2]$ ($R = Ph$, Et) were made as described previously.³

Dimethyldigold(I,III) Complexes, $[Au^{I,III}_2(CH_3)_2(\mu-2-C_6H_4PR_2)_2]$ ($R = Ph$ (2a**), Et (**2b**)).** A stirred solution of **1a** (94 mg, 0.086 mmol) or **1b** (78 mg, 0.086 mmol) in toluene (20 mL) was cooled in dry ice and treated dropwise with an ether solution of dimethylmagnesium (0.095 mmol) over 15 min. The resulting yellow solution was stirred and warmed to room temperature over 3 h. Solvents were removed in vacuo, and the residue was extracted with hexane (2×10 mL). Suspended salts were removed by centrifugation, and solvent was removed in vacuo to leave the crude product as a colorless solid, which was purified by crystallization from CH_2Cl_2 /ethanol. Yields of **2a** and **2b** were 70–80%. X-ray-quality crystals of **2a** were obtained by layering a solution in CH_2Cl_2 with 95% ethanol. **2a**: 1H NMR (CD_2Cl_2) δ 0.02 (d, $J_{PH} = 2$ Hz, CH_3); $^{31}P\{^1H\}$ NMR (CD_2Cl_2) δ 33.9 (d), 17.6 (d, $J_{PP} = 27.8$ Hz); FAB-MS m/z 931 [$M^+ - 15$]. Anal. Calcd for $C_{38}H_{34}Au_2P_2$: C, 48.22; H, 3.62. Found: C, 47.26; H, 3.20. **2b**: 1H NMR (CD_2Cl_2) δ 0.26

(21) Appleton, T. G.; Clark, H. C.; Manzer, L. E. *Coord. Chem. Rev.* **1973**, *10*, 335.

(22) Basil, J. D.; Murray, H. H.; Fackler, J. P., Jr.; Tocher, J.; Mazany, A. M.; Trczinska-Bancroft, B.; Knachel, H.; Dudis, D.; Delord, T. J.; Marler, D. O. *J. Am. Chem. Soc.* **1985**, *107*, 6908.

(23) Murray, H. H.; Fackler, J. P., Jr.; Trczinska-Bancroft, B. *Organometallics* **1985**, *4*, 1633.

(24) Porter, L. C.; Fackler, J. P., Jr. *Acta Crystallogr., Sect. C* **1986**, *42*, 1128.

(25) Talay, R.; Rehder, D. *Z. Naturforsch., B* **1981**, *36*, 459.

(26) Tunney, S. E.; Stille, J. K. *J. Org. Chem.* **1987**, *52*, 748.

(27) Harder, S.; Brandsma, L.; Kanters, J. A.; Duisenberg, A.; van Lenthe, J. *J. Organomet. Chem.* **1991**, *420*, 143.

(28) Hart, F. A. *J. Chem. Soc.* **1960**, 3324.

(29) Andersen, R. A.; Wilkinson, G. *Inorg. Synth.* **1979**, *19*, 262.

Table 4. Crystal and Refinement Data for Compounds **2a**, **4a**, **5a**, **5b**, **6a**, and **10b**

	2a	3a	4a	4b	5a	10b
chem formula	C ₃₈ H ₃₄ Au ₂ P ₂	C ₄₈ H ₂₈ Au ₂ F ₁₀ P ₂	(a) Crystal Data C ₄₈ H ₂₈ Au ₂ F ₁₀ P ₂	C ₃₂ H ₂₈ Au ₂ F ₁₀ P ₂	C ₄₈ H ₂₈ Au ₂ F ₁₀ P ₂ · 0.75C ₃ H ₆ O	C ₂₂ H ₂₈ Au ₂ N ₂ P ₂ S ₂
fw	946.57	1250.61	1250.61	1058.44	1294.17	840.48
cryst syst	triclinic	monoclinic	monoclinic	monoclinic	monoclinic	monoclinic
unit cell dimens						
<i>a</i> (Å)	9.414(2)	11.856(3)	16.588(6)	18.403(1)	18.534(6)	9.685(3)
<i>b</i> (Å)	11.173(2)	15.330(4)	12.275(5)	8.322(2)	21.930(6)	23.091(7)
<i>c</i> (Å)	16.567(2)	23.551(5)	21.166(4)	22.104(2)	22.122(1)	11.999(4)
α (deg)	106.97(1)					
β (deg)	94.32(2)	94.34(2)	90.76(2)	90.314(6)	93.04(2)	99.86(3)
γ (deg)	99.98(2)					
<i>V</i> (Å ³)	1626.8(6)	4268(1)	4309(2)	3384.9(7)	8979(4)	2644(1)
space group	<i>P</i> 1 (No. 2)	<i>P</i> 2 ₁ / <i>n</i> (No. 14)	<i>P</i> 2 ₁ / <i>c</i> (No. 14)	<i>C</i> 2/ <i>c</i> (No. 15)	<i>P</i> 2 ₁ / <i>n</i> (No. 14)	<i>P</i> 2 ₁ / <i>n</i> (No. 14)
<i>D</i> _c (g cm ⁻³)	1.93	1.95	1.93	2.08	1.915	2.11
<i>Z</i>	2	4	4	4	8	4
<i>F</i> (000)	900.0	2376.0	2376.0	1992.0	4944.0	1576.00
color, habit	colorless, prism	yellow, parallelepiped	yellow, prism	colorless, needle	colorless, needle	colorless, block
cryst dimens (mm)	0.14 × 0.07 × 0.16	0.28 × 0.12 × 0.09	0.28 × 0.26 × 0.10	0.44 × 0.08 × 0.07	0.30 × 0.09 × 0.05	0.31 × 0.21 × 0.19
μ (cm ⁻¹)	175.4 (Cu K α)	70.4 (Mo K α)	69.8 (Mo K α)	179.2 (Cu K α)	132.7 (Cu K α)	114.2 (Mo K α)
(b) Data Collection and Processing						
diffractometer	Rigaku AFC6R	Philips PW1100/20	Rigaku AFC6S	Rigaku AFC6R	Rigaku AFC6R	Philips PW1100/20
X-radiation	Cu K α	Mo K α	Mo K α	Cu K α	Cu K α	Mo K α
<i>T</i> (°C)	23(1)	20(1)	23(1)	23(1)	23(1)	23(1)
scan mode	ω -2 θ	ω -2 θ	ω -2 θ	ω -2 θ	ω -2 θ	ω -2 θ
ω -scan width (deg)	1.10 + 0.30 tan θ	1.00 + 0.35 tan θ	0.80 + 0.34 tan θ	1.20 + 0.30 tan θ	1.20 + 0.30 tan θ	0.90 + 0.34 tan θ
2 θ _{max} (deg)	120.3	50.0	50.1	120.1	120	55.0
no. of rflns						
unique	4824	7830	8039	2527	10 865	6271
obsd	4529 (<i>I</i> > 3 σ (<i>I</i>))	4874 (<i>I</i> > 3 σ (<i>I</i>))	3500 (<i>I</i> > 3 σ (<i>I</i>))	1829 (<i>I</i> > 2 σ (<i>I</i>))	6406 (<i>I</i> > 3 σ (<i>I</i>))	3480 (<i>I</i> > 3 σ (<i>I</i>))
abs cor	analytical	analytical	ψ -scan	analytical	ψ -scan	analytical
transmissn factors	0.11–0.37	0.32–0.44	0.78–1.00	0.10–0.35	0.315–0.515	0.14–0.26
(c) Structure Analysis and Refinement						
struct soln	Patterson methods		full-matrix least squares		direct methods	
refinement						
no. of params	380		559		275	
weighting	[$\sigma^2(F) + (6.4 \times 10^{-5})F^2$] ⁻¹		[$\sigma^2(F) + (2.25 \times 10^{-6})F^2$] ⁻¹		[$\sigma^2(F) + (9 \times 10^{-4})F^2$] ⁻¹	
scheme <i>w</i>						
<i>R</i> (obsd) (%)	3.5		3.8		5.4	
<i>R</i> _w (obsd) (%)	4.7		2.4		7.4	
GOF	3.79		1.48		1.49	
max/min peak	1.73/–2.54		1.67/–1.21		2.1/–1.70	
in final						
diff map (e Å ⁻³)						

(d, $J_{\text{PH}} = 2$ Hz, AuCH₃), 1.15 (sym 8-line pattern, PCH₂CH₃), 2.0–2.4 (overlapping m, PCH₂); ³¹P{¹H} NMR (CD₂Cl₂) δ 33.6 (d), 7.0 (d, $J_{\text{PP}} = 27.5$ Hz); FAB-MS *m/z* 739 [M⁺ – 15]. Anal. Calcd for C₂₂H₃₄Au₂P₂: C, 35.03; H, 4.54. Found: C, 35.10; H, 4.79.

Attempted Reaction of [Au^{III}₂(CH₃)₂(μ -2-C₆H₄PPh₂)₂] (2a) with Benzoic Acid. In an NMR tube, a solution of **2a** (13 mg, 0.014 mmol) in CD₂Cl₂ (0.6 mL) was treated with benzoic acid (2 mg, 0.016 mmol) and the course of reaction was monitored by ³¹P NMR spectroscopy. After 2 h a singlet at δ 36.3 had appeared, presumably due to [Au₂(μ -2-C₆H₄-PPh₂)₂] formed by reductive elimination of ethane. After 24 h a singlet at δ 4.6 due to the bis(benzoato) complex **1a** was also evident and, after 48 h, these two peaks, in a ratio of ca. 2:1, had completely replaced those due to **2a**.

A similar reaction in which **2a** was treated with an excess of benzoic acid gave, after 48 h, mainly **1a**, a small amount of [Au₂(μ -2-C₆H₄PPh₂)₂], and a small amount of unidentified decomposition products. There was no evidence for the formation of a methyl benzoato complex, [Au₂(CH₃)(O₂CPh)(μ -2-C₆H₄-PPh₂)₂].

Bis(pentafluorophenyl)digold(II) Complexes, [Au^{II}₂(C₆F₅)₂(μ -2-C₆H₄PR₂)₂] (R = Ph (3a), Et (3b)). A solution of C₆F₅Br (0.069 mL, 0.55 mmol) in ether (25 mL) was cooled in dry ice and treated dropwise with a 1.6 M solution of *n*-butyllithium in hexane (0.35 mL, 0.55 mmol). The mixture was stirred at dry ice temperature for 1 h, and the resulting solution of C₆F₅Li was treated over a 30 min period with a solution of **1a** (252 mg, 0.23 mmol) or **1b** (208 mg, 0.23 mmol) in toluene (50 mL), the temperature being maintained at ca. –70 °C. After being stirred for a further 30 min, the mixture was warmed to room temperature and was stirred for 3 h. The

yellow solution was filtered through Celite in air, and the solvent was removed in vacuo. The crude product was purified by passing a toluene solution down a short column of neutral alumina and eluting with toluene/hexane. The solvent was stripped, and the yellow residue was recrystallized from toluene/hexane to give **3a** or **3b** in yields of 80–90%. X-ray-quality crystals of **3a** were obtained by diffusion of pentane into a toluene solution. **3a**: ¹⁹F NMR (CD₂Cl₂) δ –119.0 (m, *o*-F), –160.0 (t, $J = 17$ Hz, *p*-F), –161.0 (m, *m*-F); ³¹P{¹H} NMR (CD₂Cl₂) δ –6.1 (s), (*d*₆-acetone) δ –5.1 (s), (C₆H₆) δ –5.7; FAB-MS *m/z* 1249 (M⁺). Anal. Calcd for C₄₈H₂₈Au₂F₁₀P₂: C, 46.10; H, 2.26. Found: C, 46.43; H, 2.04. **3b**: ¹H NMR (C₆D₆) δ 0.83 (dt, PCH₂CH₃), 1.86 (m, CH₂); ¹⁹F NMR (C₆D₆) δ –119.2 (d, $J = 24$ Hz, *o*-F), –158.1 (t, $J = 21$ Hz, *p*-F), –159.8 (t, $J = 23$ Hz, *m*-F); ³¹P{¹H} NMR (CD₂Cl₂) δ –7.8 (s), (*d*₆-acetone) –6.1 (s), (C₆D₆) δ –7.9. Anal. Calcd for C₃₂H₂₈Au₂F₁₀P₂·0.5C₆H₁₄: C, 38.16; H, 3.20; P, 5.62. Found: C, 38.17; H, 3.41; P, 5.42.

The ³¹P{¹H} NMR spectrum of a CD₂Cl₂ solution containing approximately equimolar amounts of **1b** ($\delta_{\text{P}} 8.2$) and **3b** ($\delta_{\text{P}} -7.8$), measured soon after mixing, showed an AB quartet at δ 7.7 and –2.5 ($J_{\text{PP}} = 66$ Hz) in addition to the original singlets; the new species is presumed to be [Au₂(O₂CPh)(C₆F₅)(μ -2-C₆H₄-PEt₂)₂], formed by anion scrambling.

Rearrangement of [Au^{II}₂(C₆F₅)₂(μ -C₆H₄PR₂)₂] (R = Ph (3a), Et (3b)). These experiments were carried out either in NMR tubes or in 10 mL Schlenk flasks that were shielded from light. A typical preparative procedure is described.

A solution of **3a** (ca. 30 mg) in *d*₈-toluene (5 mL) was heated at 90 °C, the progress of the rearrangement being monitored by ³¹P NMR spectroscopy. The doublet of doublets assigned to the intermediate [(C₆F₅)Au(μ -2-Ph₂PC₆H₄)Au^{III}(C₆F₅)(η ²-2-C₆H₄PPh₂)] (see text) began to appear after 5 h. After 20 h,

singlets due to the C–C-coupled product $[\text{Au}^{\text{I}}_2(\text{C}_6\text{F}_5)_2(\mu\text{-}2,2'\text{-Ph}_2\text{PC}_6\text{H}_4\text{C}_6\text{H}_4\text{PPh}_2)]$ (**4a**) and the zwitterionic complex $[(\text{C}_6\text{F}_5)_2\text{-Au}^{\text{III}}(\mu\text{-C}_6\text{H}_4\text{PPh}_2)_2\text{Au}^{\text{I}}]$ (**5a**) were observed and, after 48 h, these were the only peaks present, in a ratio of 7:1. The solvent was removed in vacuo, and the residue was dissolved in a few milliliters of acetone. After several hours, X-ray-quality crystals of **5a** precipitated. The supernatant liquid was decanted and evaporated to dryness; the residue was then taken up in a few milliliters of benzene. Layering the solution with hexane produced, after several hours, X-ray-quality crystals of **4a**. **4a**: ^{19}F NMR (C_6D_6) δ -113.4 (d, $J = 28$ Hz, $\sigma\text{-F}$), -158.8 (t, $J = 20$ Hz, $\rho\text{-F}$), -162.3 (td, $J = 32$ Hz, $m\text{-F}$); $^{31}\text{P}\{^1\text{H}\}$ NMR ($d_8\text{-toluene}$) δ 36.3 (approx t, $J_{\text{PF}} = 6.3$ Hz), (C_6D_6) 36.2, ($d_6\text{-acetone}$) δ 36.8. **4b**: ^{19}F NMR (C_6D_6) δ -116.5 (m, $\sigma\text{-F}$), -161.4 (t, $J = 19.4$ Hz, $\rho\text{-F}$), -166.0 (m, $m\text{-F}$); $^{31}\text{P}\{^1\text{H}\}$ NMR (C_6D_6) δ 32.8 (approx t, $J_{\text{PF}} = 6.3$ Hz), ($d_6\text{-acetone}$) δ 34.2.

The procedure in the case of **3b** was similar except that, in $d_8\text{-toluene}$, the coupled product $[\text{Au}^{\text{I}}_2(\text{C}_6\text{F}_5)_2(\mu\text{-}2,2'\text{-Et}_2\text{PC}_6\text{H}_4\text{C}_6\text{H}_4\text{-PEt}_2)]$ (**4b**) was the almost exclusive product in the absence of light. In acetone, no precautions being taken to exclude light, a mixture of **4b** and the presumed zwitterionic complex $[(\text{C}_6\text{F}_5)_2\text{Au}^{\text{III}}(\mu\text{-C}_6\text{H}_4\text{PEt}_2)_2\text{Au}^{\text{I}}]$ (**5b**) was formed. X-ray-quality crystals of **4b** were obtained from dichloromethane/hexane. **4b**: ^{19}F NMR (C_6D_6) δ -114.7 (dt, $J = 29, 8.9$ Hz, $\sigma\text{-F}$), -158.9 (t, $J = 20$ Hz, $\rho\text{-F}$), -162.5 (m, $m\text{-F}$); $^{31}\text{P}\{^1\text{H}\}$ NMR (C_6D_6) δ 30.9 (approx t, $J_{\text{PF}} = 7.7$ Hz). Anal. Calcd for $\text{C}_{38}\text{H}_{28}\text{Au}_2\text{F}_{10}\text{P}_2$: C, 36.31; H, 2.67; P, 5.85. Found: C, 36.65; H, 3.05; P, 6.15. **5b**: $^{31}\text{P}\{^1\text{H}\}$ NMR (C_6D_6) δ 32.9 (approx t, $J_{\text{PF}} = 6.6$ Hz).

Bis(thiocyanato)digold(II) Complexes, $[\text{Au}^{\text{II}}_2(\text{SCN})_2(\mu\text{-}2\text{-C}_6\text{H}_4\text{PR}_2)_2]$ (R = Ph (8a**), Et (**8b**)).** Treatment of a solution of **1a** (306 mg, 0.028 mmol) or **1b** (253 mg, 0.028 mmol) in acetone (10 mL) with an excess of KSCN or LiSCN in acetone (5 mL) caused immediate, quantitative precipitation of **8a** or **8b** as orange solids, which were separated by filtration and washed with acetone. The solids appear to be unstable even when stored under nitrogen at 0 °C in the absence of light. **8a**: IR (cm^{-1} , KBr) 2120 vs [$\nu(\text{CN})$], 694 vs [$\nu(\text{CS})$]; (polythene) 246 vs [Au–SCN]; $^{31}\text{P}\{^1\text{H}\}$ NMR (CD_2Cl_2) δ 0.0 (s). **8b**: IR (cm^{-1} , KBr) 2126 vs, 2105 vs, (Nujol) 2128 s, 2116 s [$\nu(\text{CN})$]; ^1H NMR (CD_2Cl_2) δ 1.3 (dt, CH_3), 2.1–2.8 (m, CH_2); $^{31}\text{P}\{^1\text{H}\}$ NMR (CD_2Cl_2) δ 0.85 (s).

The $^{31}\text{P}\{^1\text{H}\}$ NMR spectrum of a solution measured immediately after mixing **8b** with $[\text{Au}_2\text{I}_2(\mu\text{-}2\text{-C}_6\text{H}_4\text{PEt}_2)_2]$ ($\delta_{\text{P}} -11.6$) in CH_2Cl_2 showed, in addition to the singlets due to the components, an AB quartet at $\delta -3.2, -7.5$ ($J_{\text{AB}} = 70$ Hz), presumably due to $[\text{Au}_2(\text{I})(\text{SCN})(\mu\text{-}2\text{-C}_6\text{H}_4\text{PEt}_2)_2]$ formed by rapid anion scrambling.

Rearrangement of $[\text{Au}^{\text{II}}_2(\text{SCN})_2(\mu\text{-}2\text{-C}_6\text{H}_4\text{PR}_2)_2]$ (R = Ph (8a**), Et (**8b**)).** Solutions of **8a** and **8b** (25–50 mg) in CD_2Cl_2 and acetone were set aside at room temperature, and the changes were monitored by ^{31}P NMR spectroscopy. After 2 h the singlets due to the starting materials had been replaced by signals assigned to $[(\text{NCS})\text{Au}^{\text{I}}(\mu\text{-}2\text{-C}_6\text{H}_4\text{PR}_2)\text{Au}^{\text{III}}(\text{SCN})(\eta^2\text{-}2\text{-C}_6\text{H}_4\text{PR}_2)]$ (R = Ph (**9a**), Et (**9b**)) and to $[\text{Au}^{\text{I}}_2(\text{SCN})_2(\mu\text{-}2,2'\text{-R}_2\text{PC}_6\text{H}_4\text{C}_6\text{H}_4\text{PR}_2)]$ (R = Ph (**10a**), Et (**10b**)). There were also singlets at δ 53.8 (R = Ph) and δ 53.3 (R = Et) of unknown origin. After 2 days, only the signals due to **10a** and **10b** remained. Exposure of a solid sample of **8a** to laboratory light for 7 days also caused complete conversion to **10a**. X-ray-quality crystals of **10a** were obtained by layering a CH_2Cl_2 solution with hexane. **9a**: $^{31}\text{P}\{^1\text{H}\}$ NMR (CD_2Cl_2) δ 38.2 (d), -49.3 (d, $J_{\text{PP}} = 11.6$ Hz). **9b**: $^{31}\text{P}\{^1\text{H}\}$ NMR (CD_2Cl_2) 37.4 (d), -41.3 (d, $J_{\text{PP}} = 11.9$ Hz). **10a**: $^{31}\text{P}\{^1\text{H}\}$ NMR (CD_2Cl_2) δ 32.0 (s); **10b**: IR (cm^{-1} , KBr) 2122 vs [$\nu(\text{CN})$]; $^{31}\text{P}\{^1\text{H}\}$ NMR ($\text{CD}_2\text{-Cl}_2$) δ 26.5 (s). Anal. Calcd for $\text{C}_{22}\text{H}_{28}\text{Au}_2\text{N}_2\text{P}_2\text{S}_2$: C, 31.44; H, 3.36; N, 3.33. Found: C, 31.93; H, 3.32; N, 3.06.

X-ray Crystallography. The crystal and refinement data for compounds **2a**, **3a**, **4a**, **4b**, **5a**, and **10b** are summarized in Table 4.

The structures of **2a** and **3a** were solved by heavy-atom Patterson methods³⁰ and those of **4a**, **4b**, and **10b** by direct methods (SIR 92).³¹ They were expanded by use of Fourier techniques.³² Non-hydrogen atoms were refined anisotropically. Hydrogen atoms were included at geometrically determined positions, which were periodically recalculated but not refined. In the case of **10b**, the terminal carbon atom C(18) of an ethyl group was disordered over two sites, which were assigned occupancy parameters of p and $1 - p$; the parameter p was refined to a final value of 0.66(2). C(18a) was assigned a fixed isotropic B value equal to the B_{eq} value of C(18). Hydrogen atoms associated with the minor orientation of the disordered ethyl group were not included. The neutral atom scattering factors were taken from ref 33; $\Delta f'$ and $\Delta f''$ values and mass attenuation coefficients were taken from ref 34. Anomalous dispersion effects were included in F_c .³⁵ Calculations were performed with the teXsan crystallographic software package;³⁶ data reduction for **3a** and **10b** was performed with XTAL 3.4.³⁷

The structure of **5a** was solved by direct methods (SHELX 86).³⁸ The unit cell contained disordered solvent regions, near 0, 0, 0 and $1/2, 0, 0$ and their equivalent positions, which could not be described properly. Their contributions to the structure factors were defined with use of back Fourier transform techniques.^{39,40} Satisfactory refinement was achieved on the basis of an asymmetric unit containing two molecules of $\text{C}_{48}\text{H}_{28}\text{-Au}_2\text{F}_{10}\text{P}_2$ related by a pseudo-translation about 0.00, 0.20, 0.48 with six disordered acetone molecules per unit cell. Only 6409 of the 10 498 independent reflections were considered reliable ($I > 3\sigma(I)$); therefore, the comprehensive constrained least-squares refinement program RAELS-96⁴¹ was used to minimize the number of parameters required to describe the structure (385 variables for 124 non-hydrogen atoms in the asymmetric unit). The Au and P atoms were refined as independent anisotropic atoms; all other atoms were refined with constraints with rigid body thermal parametrization.⁴⁰ Calculations were carried out with teXsan³⁶ and RAELS-96.⁴¹

Supporting Information Available: Full crystallographic data for **2a**, **3a**, **4a**, **4b**, **5a**, and **10b**, including tables of atomic coordinates, anisotropic displacement parameters, and bond lengths and angles. This material is available free of charge via the Internet at <http://pubs.acs.org>.

OM000773W

(30) Beurskens, P. T.; Admiraal, G.; Beurskens, G.; Bosman, W. P.; Garcia-Granda, S.; Gould, R. O.; Smits, J. M. M.; Smykalla, C. PATTY: The DIRDIF Program System; Technical Report of the Crystallography Laboratory; University of Nijmegen, Nijmegen, The Netherlands, 1992.

(31) Altomare, A.; Cascarano, M.; Giacovazzo, C.; Guagliardi, A.; Burla, M. C.; Polidori, G.; Camalli, M. *J. Appl. Crystallogr.* **1994**, *27*, 435.

(32) Beurskens, P. T.; Admiraal, G.; Beurskens, G.; Bosman, W. P.; de Gelder, R.; Israel, R.; Smits, J. M. M. The DIRDIF-94 Program System; Technical Report of the Crystallography Laboratory; University of Nijmegen, Nijmegen, The Netherlands, 1994.

(33) Cromer, D. T.; Waber, J. T. *International Tables for X-ray Crystallography*; Kynoch Press: Birmingham, U.K., 1974; Vol. IV.

(34) *International Tables for Crystallography*; Wilson, A. J. C., Ed.; Kluwer Academic: Dordrecht, The Netherlands; Vol. C.

(35) Ibers, J. A.; Hamilton, W. C. *Acta Crystallogr.* **1964**, *17*, 781.

(36) teXsan: Single-Crystal Structure Analysis Software, Version 1.8; Molecular Structure Corp., 3200 Research Forest Drive, The Woodlands, TX 77381, 1997.

(37) Hall, S. R.; King, G. S. D.; Stewart, J. M., Eds. *XTAL 3.4 Reference Manual*; University of Western Australia; Lamb: Perth, Australia, 1995.

(38) Sheldrick, G. M. In *Crystallographic Computing 3*; Sheldrick, G. M.; Krüger, C.; Goddard, R., Eds.; Oxford University Press: Oxford, U.K., 1985; pp 175–189.

(39) Rae, A. D.; Baker, A. T. *Acta Crystallogr.* **1984**, *A40*, C428 (supplement).

(40) Rae, A. D. *Acta Crystallogr.* **1975**, *A31*, 560.

(41) Rae, A. D. RAELS 96: A Comprehensive Constrained Least-Square Refinement Program; Australian National University, Canberra, ACT, Australia, 1996.